Development 126, 1211-1223 (1999)
Printed in Great Britain © The Company of Biologists Limited 1999
DEV4108



# A *Wnt5a* pathway underlies outgrowth of multiple structures in the vertebrate embryo

**Terry P. Yamaguchi[1], Allan Bradley[2], Andrew P. McMahon[1,*] and Steven Jones[2,‡]**

[1]Department of Molecular and Cellular Biology, Biological Laboratories, Harvard University, Cambridge, MA 02138, USA
[2]Howard Hughes Medical Institute, Baylor College of Medicine, Houston, TX 77030, USA
[‡]Present address: Department of Cell Biology, University of Massachussetts Medical Center, 55 Lake Avenue North, Worcester, MA 01655, USA
*Author for correspondence (e-mail: amcmahon@biosun.harvard.edu)

*Accepted 4 January; published on WWW 15 February 1999*

## SUMMARY

**Morphogenesis depends on the precise control of basic cellular processes such as cell proliferation and differentiation. *Wnt5a* may regulate these processes since it is expressed in a gradient at the caudal end of the growing embryo during gastrulation, and later in the distal-most aspect of several structures that extend from the body. A loss-of-function mutation of *Wnt5a* leads to an inability to extend the A-P axis due to a progressive reduction in the size of caudal structures. In the limbs, truncation of the proximal skeleton and absence of distal digits correlates with reduced proliferation of putative progenitor cells within the progress zone. However, expression of progress zone markers, and several genes implicated in distal outgrowth and patterning including *Distalless, Hoxd* and *Fgf* family members was not altered. Taken together with the outgrowth defects observed in the developing face, ears and genitals, our data indicates that *Wnt5a* regulates a pathway common to many structures whose development requires extension from the primary body axis. The reduced number of proliferating cells in both the progress zone and the primitive streak mesoderm suggests that one function of *Wnt5a* is to regulate the proliferation of progenitor cells.**

Key words: Axis formation, Wnt5a, Limb outgrowth, Progenitor cells, Mouse, Gastrulation

## INTRODUCTION

Understanding how the coordination of cellular proliferation and differentiation can give rise to a patterned three-dimensional tissue is a fundamental problem for developmental and evolutionary biologists. During gastrulation and tailbud extension in the vertebrate embryo, coordination of these processes is required for a considerable period of time to allocate the cells that constitute the trunk and tail along the anterior-posterior (A-P) axis. At the onset of gastrulation (6.5 days post coitum, d.p.c.), the mouse embryo consists of two germ layers, the primitive ectoderm (epiblast) and the visceral endoderm. Gastrulation converts the two germ layers into three by recruiting pluripotent epiblast cells to a transient structure known as the primitive streak. The primitive streak indicates the posterior end of the A-P axis. A large proportion of the epiblast gives rise to descendants which ingress through the streak and form the mesoderm and definitive endoderm germ layers. Later, (7.5-9.5 d.p.c.) only a small strip of epiblast adjacent to the primitive streak contributes progeny that ingress through the streak (Tam, 1989; Wilson and Beddington, 1996) yet a large number of mesoderm cells are generated that significantly participate in the caudal extension of the embryonic axis. A growing body of evidence suggests that a permanent pool of stem cells develops in the primitive streak mesoderm and that these cells may be the primary source of the mesodermal cells that constitute the embryonic trunk (Tam and Trainor, 1994 for review; Beddington, 1994; Nicolas et al., 1996; Wilson and Beddington, 1996).

Gastrulation ends in the mouse when the primitive streak disappears and ingression of superficial ectoderm ceases, the posterior neuropore closes, and the 30 somites that constitute the trunk mesoderm have formed (Wilson and Beddington, 1996). Extension of the A-P axis at these later stages is accomplished by the addition of cells furnished by the tailbud to the caudal end of the embryo. Lineage analyses demonstrate that the primitive streak and the tailbud are related structures and suggest that the paraxial mesoderm stem cells that reside in the primitive streak during gastrulation become the paraxial mesoderm progenitors that populate the tailbud (Tam and Tan, 1992; Wilson and Beddington, 1996). Thus the primitive streak is most likely the source of stem cells that give rise to the mesoderm of the entire trunk and tail. How these processes are regulated at the molecular level is unknown.

As caudal extension of the embryonic body axis proceeds, outgrowth of new structures away from the main body axis is initiated. For example, outgrowth of the maxillary component of the first branchial arch has started by the 10 somite stage, while the forelimb and hindlimb primordia bud from the lateral ridge mesoderm at the 15 somite and 25-30 somite stage,

respectively. By the 40-45 somite stages (11.5 d.p.c.) outgrowth of the genital tubercle in the ventral midline can be detected (Kaufman, 1992).

Most of our knowledge of how an outgrowing tissue becomes patterned in the vertebrate embryo has come from studies on the limb. While growth of the developing limb occurs in all dimensions, outgrowth along the proximal-distal (P-D) axis far exceeds growth along the other axes. P-D outgrowth and pattern is controlled by the apical ectodermal ridge (AER), a narrow epithelial structure localized to the distal ectodermal tip of the limb. Surgical removal of the AER results in growth cessation and truncation of the limb at an axial level dependent upon the time of AER removal; early removals generate proximal truncations while later removal leads to distal truncations (Saunders, 1948). Signals from the AER act upon the underlying mesenchymal cells of the progress zone, to maintain them in a proliferating and undifferentiated state in which positional information remains labile. The progress zone model for P-D cell fate specification proposes that the time a limb progenitor cell resides in the progress zone determines its P-D position (Summerbell et al., 1973). Once descendants leave the progress zone, positional values become fixed; cells that leave the progress zone early adopt proximal fates while cells that leave later become progressively more distal. Early progress zone cells therefore are a source of progenitor cells for later distal territories. Fibroblast growth factors (Fgf) produced by the AER and the *Hox* genes expressed in the mesenchyme likely participate in these events (Johnson and Tabin, 1997 for review).

Several *Wnt* family members representing at least two distinct functional classes of *Wnts* (Moon et al., 1997 for review) are expressed in the developing mammalian limb. *Wnt7a*, a putative member of the *Wnt1* class, is required for proper specification of the dorsal-ventral axis of the limb (Parr and McMahon, 1995), however nothing is known about the function of the *Wnt5a* class of *Wnts* during limb development. *Wnt5a* is unique in that it is the only *Wnt* expressed in the progress zone (Gavin et al., 1990; Parr et al., 1993). Furthermore, *Wnt5a* does not appear to signal via the canonical *wg/Wnt1* β-catenin-dependent signalling pathway but instead can activate a phosphatidylinositol pathway in a zebrafish assay (Slusarski et al., 1997). *Wnt5a* is expressed in a graded fashion in the distal limb mesenchyme during its outgrowth, but is also expressed in a similar fashion during the morphogenesis of the facial processes, and in the primitive streak and tailbud during the growth and extension of the embryonic A-P axis (Gavin et al., 1990; Takada et al., 1994). These observations have led us to investigate whether *Wnt5a* might have a conserved function which underlies the outgrowth of diverse embryonic structures.

## MATERIALS AND METHODS

### *Wnt5a* targeting in ES cells and creation of *Wnt5a*-deficient mice

The mouse *Wnt5a* gene was isolated from a 129-SvJ recombinant phage library (Stratagene) and gene structure was partially characterized. Genomic fragments of 3.2 kb and 2.8 kb in length flanking an *Msc*I restriction endonuclease site in exon 2 were used to create a gene replacement vector. A PGK-*neo* positive selection marker and MC1*tk* negative selection marker were included in the targeting vector (pWKOII). AB1 embryonic stem cells were electroporated with *Not*I-linearized targeting vector and selected in G418 and FIAU at 24 hours post-electroporation. Double-resistant colonies were isolated and genomic DNA was prepared and analyzed by Southern blot. Correct targeting of *Wnt5a* was indicated by the presence of a 7.3 kb fragment in an *Eco*RI/*Eco*RV double digest of genomic DNA using an *Eco*RI-*Xho*I 5′ external probe, and a 5.4 kb fragment in a *Bam*HI digest of genomic DNA using a *Xho*I-*Bam*HI 3′ external probe. Multiple ES cell clones displaying proper targeting of the *Wnt5a* allele were isolated, expanded, and microinjected into day 3.5 blastocysts (strain C57BL/6) to generate chimeric mice. Offspring of matings between chimeric and C57BL/6 mice were genotyped by Southern analysis of genomic DNA harvested from tail biopsies to identify germline transmission of the mutated *Wnt5a* allele. Subsequent intercrosses of *Wnt5a*-heterozygous mice were performed to generate *Wnt5a*-null embryos.

### Embryo collection and analysis

Embryos were dissected into PBS and fixed in 4% paraformaldehyde (for RNA in situ analysis and bromodeoxyuridine (BrdU) detection), in Bouin's fixative (for histological analysis), in 95% ethanol (for skeleton analyses) or in 1% formaldehyde/0.2% glutaraldehyde (for β-galactosidase staining). For analysis of tissue sections, embryos were processed, embedded in paraffin wax, and sectioned at 6 μm. Sections for general histology were stained with hematoxylin and eosin. All analyses were performed using previously published protocols: whole-mount and section RNA in situ hybridization according to Wilkinson and Nieto (1993), skeleton preparations according to Parr and McMahon (1995), β-galactosidase staining according to Whiting et al. (1991), anti-*Dlx* homeoprotein labelling according to Panganiban et al. (1997), and whole-mount TUNEL analysis according to Conlon et al. (1995).

### Brdu detection and cell counting

Pregnant females were injected intraperitoneally with 50 μg BrdU/gram body weight and killed 90 minutes after injection. Embryos were sectioned as described above, and BrdU was detected immunohistochemically (Nowakowski et al., 1989). Labelled sections were counterstained with 0.1% basic fuchsin (12.5 d.p.c. forelimbs) or 0.01% toluidine blue (8.5 d.p.c. embryos). 12.5 d.p.c. limbs were oriented such that sections were cut in the proximal-distal and dorsal-ventral planes. Analysis of labelled limb sections was performed by counting a 200×250 μm (D-V and P-D axes, respectively) area of immunoreactive distal mesenchymal cells lying between the AER and the distal end of the condensing mesenchyme and within the *Wnt5a* mRNA-expressing domain. No less than four sections, each separated by 18 μm or greater, from each pair of stage-matched embryo siblings ($n$=6) were counted.

Transverse sections through the caudal end of 8.5 d.p.c. embryos including the primitive streak were analysed for incorporation of BrdU. All mesenchymal cells lying between the ectoderm and the hindgut endoderm were counted. A minimum of three sections per embryo, each separated by 18 μm or greater, from each pair of stage-matched embryo siblings ($n$=3) were counted.

## RESULTS

### *Wnt5a* is expressed in multiple outgrowing tissues

*Wnt5a* is strongly expressed in the caudal end of the embryo for seven gestational days during the stages when growth and patterning of the embryonic A-P axis occurs. Transcripts are found in a graded fashion along the A-P axis during all gastrulation stages (6.5-9.5 d.p.c.) with highest levels expressed in the mesoderm of the caudal primitive streak and the allantois, diminishing to lower levels in the anterior streak and in mesoderm lateral to the streak (Fig. 1a; Takada et al.,

1994). As somitogenesis commences (8.0 d.p.c.), high transcript levels are maintained in the primitive streak and the caudal lateral and paraxial presomitic mesoderm (PSM). The rostral limit of *Wnt5a* expression in the caudal paraxial mesoderm is difficult to establish since transcript levels diminish gradually, however *Wnt5a* has not been detected in the newly formed somite (Fig. 1b). This pattern is maintained in the caudal end of the embryo during tailbud stages (10.0-13.5 d.p.c.) as *Wnt5a* is expressed in the tailbud (Fig. 1d; Takada et al., 1994) and in the caudal end of all three germ layers including the hindgut endoderm (Gavin et al., 1990; data not shown). *Wnt5a* is also expressed in mesenchyme of the developing gut at 10.5 and 12.5 d.p.c. (Fig. 1d,i).

*Wnt5a* is detected in association with facial development in the outgrowing first branchial arch by the 14-16 somite stage (Fig. 1b; Takada et al., 1994). By 9.5 d.p.c., it is highly expressed in a graded fashion in the outgrowing regions of the facial primordia including the frontonasal process and the maxillary and mandibular components of the first branchial arch (Fig. 1c). This graded expression in the developing face, as well as in the tongue, continues until at least 12.5 d.p.c. (Fig. 1i).

In the limb, *Wnt5a* expression is first observed just after the forelimb has started to bud around 20-22 somites. At this point transcripts are localised to the ventral limb ectoderm, and shortly thereafter to the early AER (Fig. 1c; Gavin et al., 1990; Parr et al., 1993). As the limb bud elongates distally, *Wnt5a* continues to be expressed in the AER but expression in the limb mesenchyme becomes graded (Fig. 1d). The highest levels occur distally, directly underlying the AER; expression tapers-off proximally. By 11.5 d.p.c., ectodermal expression is down-regulated and graded transcripts are confined to the distal mesenchyme (Fig. 1e; Gavin et al., 1990). Upon condensation of the digit primordia at 12.5 d.p.c., *Wnt5a* mRNA becomes excluded from the core mesenchyme (Fig. 1f), but is expressed in the perichondrium of the limb skeleton, and in mesenchyme cells adjacent to the perichondrium (Fig. 1j). Perichondrial expression is prominent throughout the developing embryonic skeleton at this stage, including the vertebral column and the trachea (Fig. 1i). At 14.5 d.p.c., whole-mount hybridizations reveal that *Wnt5a* is expressed strongly in the distal two-thirds of the digit perichondrium (Fig. 1g). Sectioned hybridizations clearly demonstrate that *Wnt5a* continues to be expressed in the perichondrium of more proximal elements such as the radius and ulna (data not shown). Similar expression patterns are observed during hindlimb development.

High levels of *Wnt5a* expression are also found in the genital primordia at 10.5 d.p.c. (Fig. 1d). Expression is graded along the outgrowing axis of the genital tubercle, with highest levels distally, as described for the limb (Fig. 1i). This expression pattern persists until at least 14.5 d.p.c. (Fig. 1h). Finally, *Wnt5a* is also expressed in a distal-to-proximal gradient in the mesenchyme cells of the pinna or outer ear (data not shown). Thus, expression of *Wnt5a* is graded along the outgrowing embryonic axis during the elaboration of the primary body

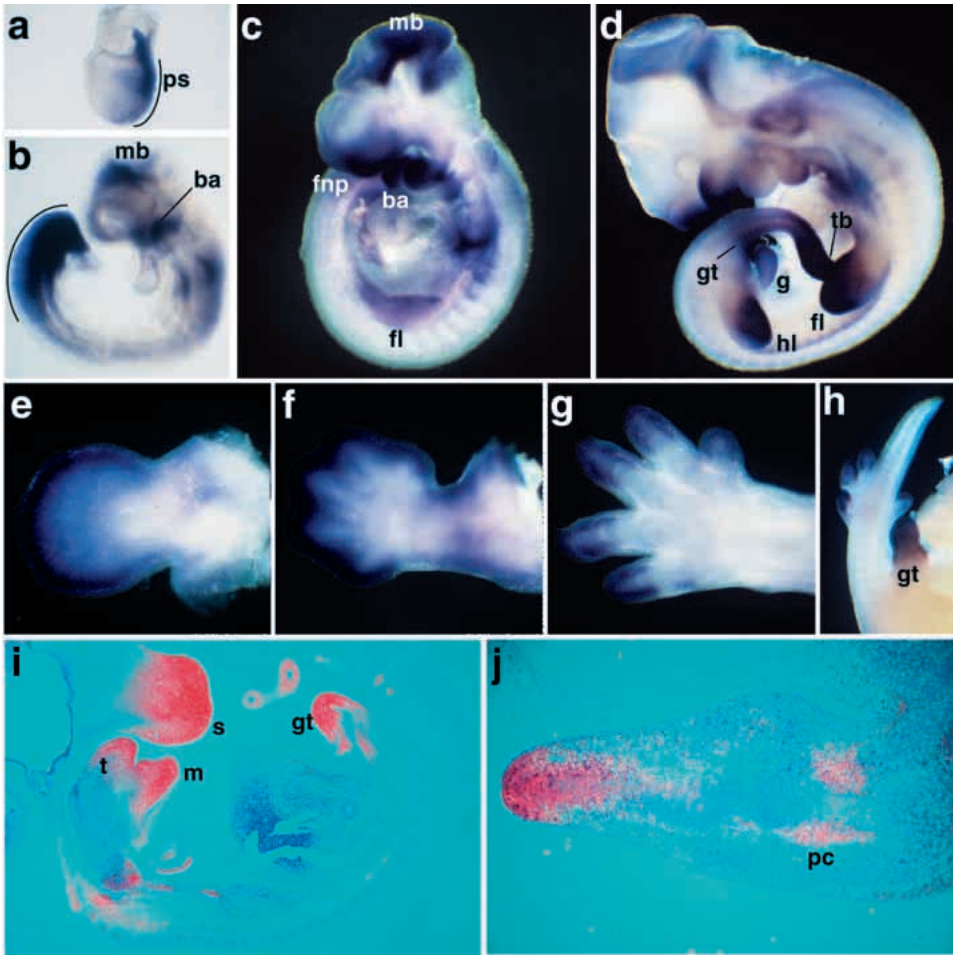


**Fig. 1.** Expression of *Wnt5a* during gastrulation, limb, face and genital development. See text for details of expression pattern. (a-h) Wholemount in situ hybridizations, i and j show in situ hybridizations performed on sectioned tissue. (a-d) Lateral views of (a) 7.5 d.p.c. embryo, anterior is to the left, (b) 8.75 d.p.c. embryo, (c) 9.5 d.p.c. embryo, (d) 10.5 d.p.c. embryo. Curved bars in a and b indicate the length of the primitive streak, and the length of the streak and PSM, respectively. (e-g) Dorsal views of limbs dissected on (e) 11.5 d.p.c., (f) 12.5 d.p.c., and (g) 14.5 d.p.c. (h) Lateral view of 14.5 d.p.c. genital tubercle. (i) Mid-sagittal section of 12.5 d.p.c. embryo. (j) Section through 12.5 d.p.c. forelimb indicating weaker *Wnt5a* expression in the ulna perichondrium relative to the strong distal expression domain. Abbreviations: (ps) primitive streak; (mb) midbrain; (ba) first branchial arch; (fnp) frontonasal process; (fl) forelimb; (gt) genital tubercle; (g) gut; (hl) hindlimb; (tb) tailbud; (t) tongue; (m) mandible; (s) snout; (pc) perichondrium.

plan, and during the development of the limb, genitals, face and pinna, suggesting that *Wnt5a* plays a conserved role in regulation of growth and pattern in multiple tissues.

### *Wnt5a* is required for morphogenesis of all outgrowing structures

To address the function of *Wnt5a* in the morphogenesis of these tissues, we functionally inactivated *Wnt5a* by gene targeting (Fig. 2). The targeted allele is likely a null since the gene is disrupted in exon 2, at codon 31 of the Wnt5a protein. Mice heterozygous for this allele had no apparent mutant phenotype. Homozygous mutant offspring of heterozygous intercrosses were born but died shortly thereafter. Thus, loss of *Wnt5a* function leads to perinatal lethality.

Analysis of late embryonic stage (17.5-18.5 d.p.c.) homozygotes revealed gross morphological defects in outgrowing tissues. Embryos were truncated caudally, displaying a loss of the tail and a significant shortening of the embryonic A-P axis (Fig. 3a,b). The shape of the mutant head appeared abnormal, suggestive of possible defects in brain morphogenesis where *Wnt5a* is expressed from early somite stages (Fig. 1b,c). The snout, mandible and tongue were truncated, and reduced outgrowth of the external ear was apparent. Both fore- and hindlimbs lacked digits, and were significantly shortened along the P-D axis (Fig. 3a-d). Finally, the genital tubercle was absent (Fig. 3c,d). Interestingly, the phenotypes observed in many tissues are similar as affected structures lack distal elements and the remaining structures are shortened along the outgrowing axis. This suggests that a common mechanism may regulate the patterning of outgrowing tissues. As more is known about the development of the body axis and the limb, we have primarily focused on these phenotypes.

### *Wnt5a* is required for extension of the primary embryonic A-P axis

A general examination of the homozygous *Wnt5a* mutant skeletons at 17.5-18.5 d.p.c. ($n$=6) revealed that the axial skeleton is abnormal. Ribs and vertebrae are often fused. The length of the mutant vertebral columns are 1/2 the length of their wild-type littermates (Fig. 4a,b). Vertebrae are generally dysmorphic and smaller in size, and abnormalities increase in severity caudally. As in wild type, 7 cervical vertebrae are always present. While 13 thoracic, 6 lumbar, 4 sacral, and approximately 30 tail vertebrae exist in wild-type vertebral columns, 12-13 thoracic vertebrae and ribs, and 5-6 lumbar vertebrae are present in the *Wnt5a* mutants. 0-4 partially fused sacral vertebrae can be identified in the mutant skeletons and no more than 4 highly abnormal, fused tail vertebrae have ever been observed. Thus, the reduced length of the mutant vertebral column is due to both the absence of caudal vertebrae and to a reduction in size of the remaining vertebrae.

The vertebrae and ribs are directly descended from the sclerotomal component of the somites. We were therefore interested in determining whether the smaller vertebrae observed in the *Wnt5a* mutants could be due to formation of smaller somites. Mutant and wild-type embryos were examined at 9.5 d.p.c. when 18-22 somites have formed. While the 7 rostral-most somites of mutants are similar in size to those of wild-type embryos, the caudal 15 become progressively

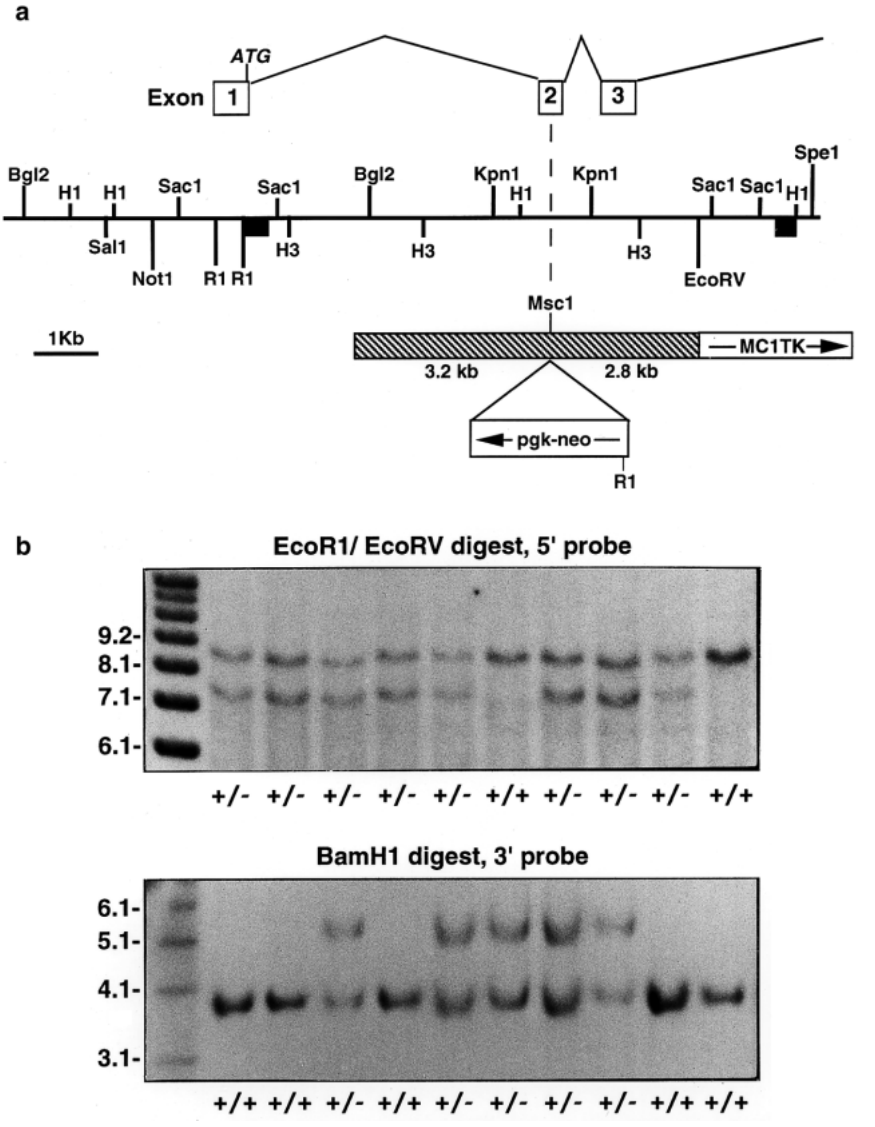


**Fig. 2.** Gene targeting at the *Wnt5a* locus. (a) Schematic representation of part of the *Wnt5a* locus and the replacement vector. Thick bars indicate the site of flanking probes used for Southern analysis and hatched area indicates region of homology in targeting vector with *Wnt5a*. (b) Southern blot analysis of targeted ES cell lines. Correct targeting of *Wnt5a* is indicated by the presence of a 7.3 kb fragment in an *Eco*RI/*Eco*RV double digest of genomic DNA using an *Eco*RI-*Xho*I 5′ flanking probe, and a 5.4 kb fragment in a *Bam*HI digest of genomic DNA using a *Xho*I-*Bam*HI 3′ flanking probe. Abbreviations: (HI) *Bam*HI, (H3) *Hin*dIII, (RI) *Eco*RI.

smaller (Fig. 3g,h). Measurements of the A-P length of the newly formed somite (somite I) of stage-matched 18-22 somite mutant embryos (Fig. 3j) indicated that they averaged 69% (±5%; *n*=4) of the length of an equivalent wild-type somite (Fig. 3i). Newly formed somites were also often reduced in size along the D-V axis although this was not consistently observed at this stage. Thus the vertebral column defects may arise, at least in part, from reduced somite size. In addition to the smaller somites, the PSM is also greatly reduced in the absence of *Wnt5a*. The A-P length of the mutant PSM was 57% (±8%; *n*=4) of the length of wild-type PSM (Fig. 3i,j). Since *Wnt5a* is expressed in the primitive streak and PSM, but not in the somites themselves at this stage, the reduction in somite size is likely due to a requirement for *Wnt5a* in somite precursors residing in the streak and PSM.

The size of the PSM normally changes during somitogenesis and axis extension. Its size is governed by a balance between the removal of cells at the rostral end to form a new somite and the addition of paraxial mesoderm cells at the caudal end of the PSM furnished by the primitive streak or the tailbud. The rate of segmentation of the PSM was unchanged by the absence of *Wnt5a* since approximately the same number of somites were observed in 4 pairs of mutant and wild-type littermates (Fig. 3g,h). Therefore, we determined whether defects in the primitive streak could account for the reduced size of the mutant PSM. Analysis of the primitive streaks of *Wnt5a* mutants revealed that the streak appears shortened or truncated at 8.5 d.p.c. (Fig. 3e,f), and this defect can be observed as early as 7.75 d.p.c. (see Fig. 5h).

The smaller PSM and shortened primitive streak observed in *Wnt5a* mutants could be due to a failure to specify caudal paraxial mesoderm. Alternatively, *Wnt5a* could function to regulate the migration of mesoderm progenitors out of the streak, or specify the regional identity of the streak. To test these possibilities, we analysed mutants for the expression of genes known to function in these processes. *Fgf8* is expressed in the primitive streak (Crossley and Martin, 1995) and is required for the formation of embryonic mesoderm (Meyers et al., 1998). *Tbx6* is expressed in both the streak and paraxial presomitic mesoderm and is essential for caudal paraxial mesoderm specification (Chapman and Papaioannou, 1998). Both continue to be expressed at normal levels in mutants at 8.5 d.p.c. suggesting that paraxial mesoderm fate continues to be specified in the absence of *Wnt5a* (Fig. 5a,b and data not shown). To test whether *Wnt5a* regulates the morphogenetic movements of mesoderm out of the streak we analysed mutants for the expression of the transcription factor *Brachyury (T)*, a gene required for these movements (Wilson et al., 1995). *Brachyury* is expressed at normal levels in the primitive streak in the absence of *Wnt5a* (Fig. 5c,d) suggesting that mesoderm migration is not significantly perturbed. *Brachyury* expression in the rostral mutant notochord is normal (arrow, Fig. 5c,d) but *Sonic hedgehog* transcripts, which are abundantly expressed in the wild-type notochord but not in the streak, indicate that a thickening of the caudal notochord has arisen in the mutant

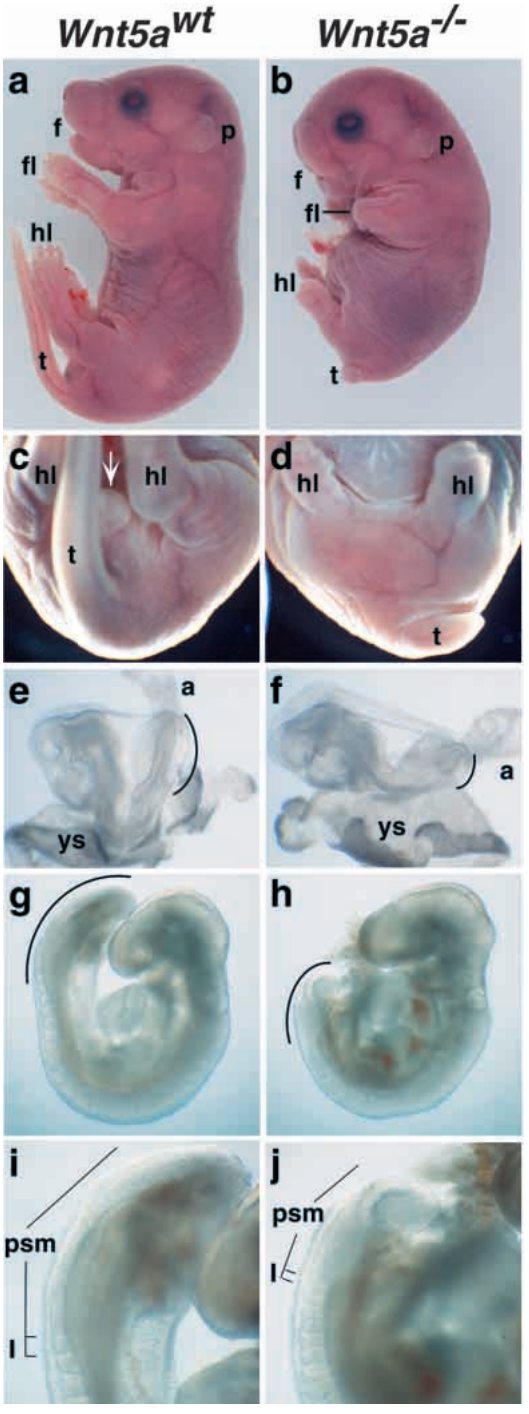


**Fig. 3.** Phenotype of *Wnt5a*$^{-/-}$ mutants. (a,b) Lateral views of wild-type and mutant embryos at 18.5 d.p.c. Note the abnormal outgrowth of the face, limbs and tail and the overall shortening of the embryonic A-P axis and the P-D axis of the limbs. (c,d) Ventral views of the caudal end of the wild-type and mutant 18.5 d.p.c. embryos. Arrow indicates the wild-type external genitalia, which are missing from the *Wnt5a*$^{-/-}$ homozygote. (e,f) Lateral views of 8.5 d.p.c. wild-type and mutant embryos. (g) Low power lateral view of a wild-type 22 somite embryo. (h) Similar view of a *Wnt5a*$^{-/-}$ 22 somite sibling. Curved bars in (e-h) indicate the reduced size of the primitive streak and presomitic mesoderm in mutant embryos compared to wild type. (i,j) High power views of the caudal end of the embryos depicted in g and h taken at the same magnification. Note the dramatic reduction in the length of the psm and somite I in the A-P axis. Abbreviations: (f) facial structures; (fl) forelimb; (hl) hindlimb; (t) tail; (p) pinna; (a) allantois; (ys) yolksac; (psm) presomitic mesoderm; (I) most recently formed somite.

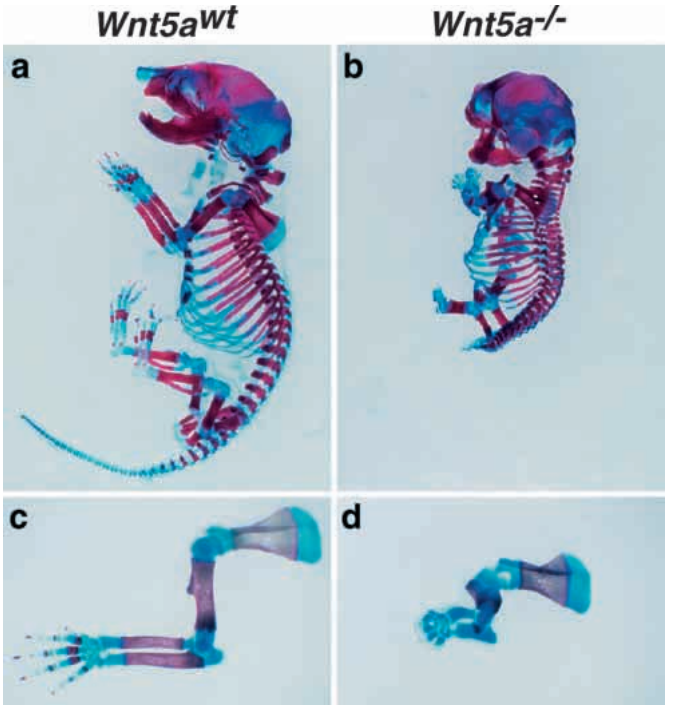


**Fig. 4.** Analysis of skeletons of *Wnt5a*$^{-/-}$ 18.5 d.p.c. embryos. Alcian Blue and Alizarin Red stained skeletons of a wild-type (a) and *Wnt5a*$^{-/-}$ (b) embryo. (c,d) High power lateral views of dissected wild-type (c), and *Wnt5a*$^{-/-}$ (d) forelimbs.

tailbud by 10.5 d.p.c. (data not shown). A large clump of *Brachyury*-positive cells were observed ventral to the streak, however these cells likely arise due to abnormal extension of the hindgut (data not shown) and thickening of caudal notochord.

Next, we investigated whether the expression of genes thought to function in regional specification of positional information in the streak and caudal body axis are altered in *Wnt5a* mutants. *Evx1* is found at one end of the *Hoxa* cluster and, like *Wnt5a*, is expressed throughout the length of the streak in a graded fashion (Bastian and Gruss, 1990; Dush and Martin, 1992). Analysis of mutant embryos at pre-somite stages indicates that *Evx1* continues to be expressed throughout the shortened mutant streak (Fig. 5g,h). Similar results were obtained with probes for *delta-like-1* (Bettenhausen et al., 1995), *lunatic fringe* (Johnston et al., 1997) and *Bmp4* (Winnier et al., 1995) (data not shown). Finally, a Lef1/β-catenin complex is implicated in the transcriptional mediation of at least some Wnt signals (Clevers and van de Wetering, 1997 for review). In *Wnt5a* mutants, *Lef1* expression in the streak and PSM is not reduced (Fig. 5e,f). Thus, *Lef1* is not a transcriptional target of Wnt5a. Taken together, all markers of the streak or presomitic mesoderm continue to be expressed, and expression is appropriately localized in the reduced caudal region of *Wnt5a* mutants. As the primitive streak and PSM appears to be correctly patterned along the A-P axis, these results indicate that the phenotype does not result from a simple loss of regional identity.

The observed truncation of the mutant tail could arise from premature loss of the tailbud. Examination of embryos at 10.5-12.5 d.p.c. demonstrated that the expression of several tailbud markers such as *Fgf8* (Fig. 5i,j), *Wnt5a*, *Hoxd11*, *d12*, *d13*, *Hoxa13* (Capecchi, 1997 for review), and *Lef1* (Oosterwegel et al., 1993), were all similar in wild-type and mutant tailbuds (data not shown). *Evx1* also continued to be expressed in the mutant tail at 10.5 d.p.c., however the expression domain was ventrally displaced, probably due to kinking of the neural tube caused by aberrant caudal axis extension (Fig. 5k,l). Interestingly, *Fgf4* expression in the caudal tip of the tailbud (Niswander and Martin, 1992), was up-regulated in the absence of *Wnt5a* (Fig. 5m,n), while the domain of *Gbx2* expression (Wassarman et al., 1997) in the paraxial presomitic mesoderm of the mutant tailbud was considerably reduced (Fig. 5o,p). Taken together with the observation that somites can be found at the very caudal tip of the mutant tail (data not shown), our data suggests that the tailbud is present in the *Wnt5a* mutants, but that by 10.5 d.p.c. most of the available paraxial mesoderm has been segmented into somites and the generation of new paraxial mesoderm has prematurely terminated.

To investigate whether the reduced A-P somite length could be due to the loss of a somite compartment, we analysed mutant embryos for the expression of genes that mark different A-P somitic domains. *Fgf4* expression is confined to a central domain within each myotome at 10.5 d.p.c. (Fig. 5q; Niswander and Martin, 1992). In *Wnt5a* mutants, expression is observed but the spacing between adjacent somitic regions is reduced as expected (Fig. 5r). In addition, sporadic ventral fusions occur between adjacent *Fgf4*-positive somites (indicated by bars in Fig. 5r). In contrast to *Fgf4*, *Fgf8* transcripts are restricted to anterior and posterior compartments of the myotome (Crossley and Martin, 1995), and are similarly restricted in the *Wnt5a* mutant somites despite their significantly smaller size (Fig. 5i,j). Thus, A-P polarity in the myotome appears normal suggesting that the loss of an A-P somitic compartment cannot account for the reduced somite length.

### *Wnt5a* is essential for outgrowth of the limb P-D axis

Examination of the *Wnt5a*$^{-/-}$ limb skeletons at 18.5 d.p.c. demonstrates severe and progressive reductions in the lengths of the individual skeletal elements along the P-D axis, culminating in the absence of the distal phalanges (Fig 4c and d). While the length of the scapula is only mildly affected, the mutant humerus is 59% the length of the wild-type limb, and the radius and ulna are only 30 and 40% ($n$=4) of their normal length, respectively. Alizarin red staining in the mutant humerus indicates that calcification is initiated in the absence of *Wnt5a*, however the morphology of the ossification center and the deltoid tuberosity are aberrant. The deposition of calcified matrix is clearly reduced in the mutant ulna and completely absent in the radius and metacarpals. Thus proximal limb elements are reduced in length and delayed in development. Although the carpals appear relatively normal, five distal chondrogenic condensations that constitute the metacarpals are present but display abnormal morphology and no digits are formed. The metacarpals in mutants are much shorter and rounder than the cylindrical wild-type metacarpals and often are partially fused with a neighbour (Fig. 4d). Thus, there is an absolute requirement for *Wnt5a* for morphogenesis of the distal-most limb elements.

To examine how this phenotype emerges, we analysed skeleton formation in *Wnt5a* mutants expressing a *lacZ*

reporter under the control of *Noggin* regulatory elements. As this reporter is active in chondrogenic mesenchyme as soon as condensation begins, this allows the earliest aspects of skeletogenesis to be followed (Brunet et al., 1998). In mutant embryos the anlage of the proximal limb primordia, the humerus, radius, and ulna, form at the appropriate time and do not appear to be reduced at 11.5 d.p.c. suggesting that their formation is independent of *Wnt5a* action (Fig. 6a,b). In contrast, the distal digit primordia which are forming at 12.0 d.p.c. have abnormal morphology and fail to extend distally (Fig. 6c,d). By 13.0 d.p.c. it is clear that none of the skeletal elements extend along the P-D axis normally when compared to stage-matched controls (Fig. 6g,h). Note that at all stages examined in this experiment the mutant progress zone (ie. distal undifferentiated β-gal-negative cells) appears to remain the same size while the wild-type progress zone becomes progressively smaller as cells leave and contribute to outgrowing digits (curved bars in Fig. 6a-h).

The reduced size of the limb skeleton along the entire P-D axis, together with the loss of distal structures, suggests that early deficiencies in the function of the AER or in the progress zone may account for the observed phenotype. To investigate the ontogeny of the mutant phenotype we examined the morphology of mutant forelimbs at 10.5-12.5 d.p.c. for expression of genes characteristic of, and necessary for, AER or progress zone function. Fgf8 is implicated in regulating P-D outgrowth and is highly expressed in the AER (Crossley and Martin, 1995; Crossley et al., 1996). Fgf8 is strongly expressed in the AER of mutants at 10.5 d.p.c. (data not shown), and expression is indistinguishable from wild-type AER at 11.5 and 12.5 d.p.c. (Fig. 7a,e). Gross morphological differences in the autopods (hand and wrist, ankle and foot) first become

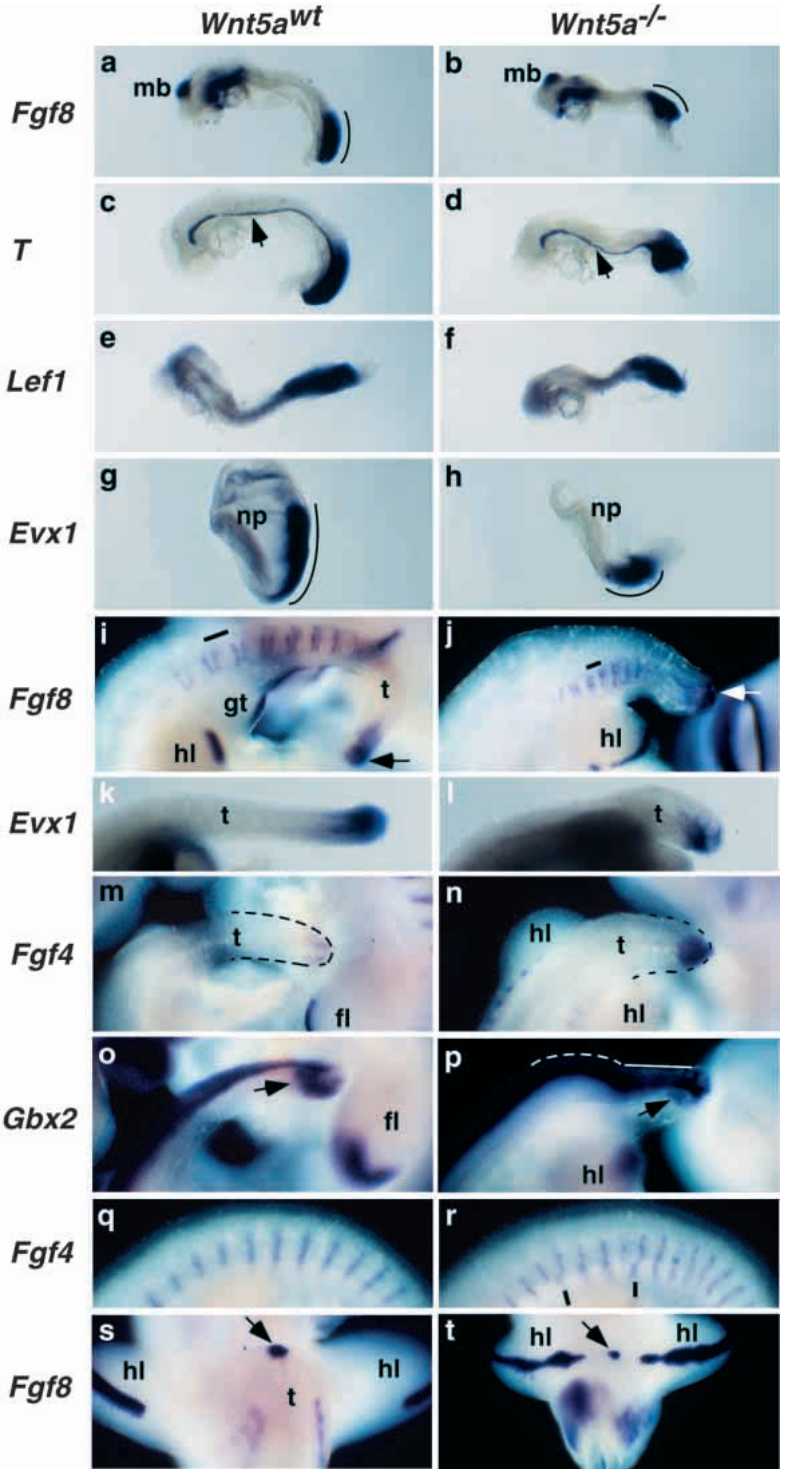


**Fig. 5.** Whole-mount in situ hybridization analysis of *Wnt5a*$^{-/-}$ 7.75-10.5 d.p.c. embryos for expression of genes that regulate gastrulation, somitogenesis and genital tubercle development. (a-r) Lateral views of wild-type (left) and *Wnt5a*$^{-/-}$ (right) embryos; anterior end of the embryo is left and the dorsal side is up. (a,b) *Fgf8* is required for embryonic mesoderm formation and continues to be expressed in 8.5 d.p.c. primitive streaks lacking *Wnt5a*. Curved bars indicate the length of the primitive streak and PSM. (c,d) *Brachyury (T)* expression in the *Wnt5a*$^{-/-}$ notochord is normal, but abnormalities exist in the caudal end of the embryo. The arrow indicates the notochord. (e,f) *Lef1* continues to be expressed in the 8.5 d.p.c. *Wnt5a*$^{-/-}$ embryo. (g,h) Graded *Evx1* expression persists in the caudal end of the 7.75 d.p.c. *Wnt5a*$^{-/-}$ embryo indicating that the primitive streak (curved bar) is likely patterned properly but considerably smaller than the wild-type streak. (i,j) *Fgf8* continues to be expressed in the tailbud (arrows) at 10.5 d.p.c., and in anterior and posterior compartments of the caudal somitic myotome. The bar indicates the length of one caudal somite. (k,l) *Evx1* is expressed in the mutant tailbud. (m,n) *Fgf4* is expressed at low levels in the wild-type 10.5 d.p.c. tailbud, however, expression is up-regulated in the *Wnt5a*$^{-/-}$ tailbud. (o,p) *Gbx2* continues to be expressed in the thickened caudal neural tube of the mutant, but the domain of paraxial mesoderm expression is reduced (arrow). Dashed lines indicate the dorsal aspect of the embryo. (q,r) *Fgf4* expression in wild-type and *Wnt5a*$^{-/-}$ embryos indicates that the myotome develops, but that ventral somitic abnormalities and fusions (black bars) arise in the absence of *Wnt5a*. (s,t) *Fgf8* is expressed at the distal tip of the outgrowing wild-type genital tubercle (arrow). The tail has been removed for clarity. A spot of *Fgf8* expression is also detected in the *Wnt5a*$^{-/-}$ midline (arrow) between the two rows of *Fgf8* expression in the mutant hindlimb AER. Abbreviations: (mb) midbrain; (np) neural plate; (t) tail; (hl) hindlimb; (gt) genital tubercle; (fl) forelimb.

discernible at 11.5 d.p.c. and obvious by 12.5 d.p.c. At these times, *Hoxa13* and *Hoxd13* are strongly expressed in the distal limb and function in a partially redundant manner to regulate the proliferation and differentiation of the skeletal primordia that constitute the autopod (Dolle et al., 1993; Fromental et al., 1996). Similarly, *Hoxa11* and *Hoxd11* are required in a partially redundant way for the growth of the radius and ulna (the zeugopod) (Davis et al., 1995). Surprisingly, these genes continue to be expressed in their normal domains and at normal levels in *Wnt5a* mutants (Fig. 7b,c, f and data not shown). However at 12.5 d.p.c. there is a failure to recruit expressing cells into digit primordia (Fig. 7f). Several genes are expressed in the distal-most mesenchyme including the progress zone and are thus candidate genes for regulation of limb outgrowth and patterning. These include members of the *Dlx* family which control P-D outgrowth in many insect appendages (Panganiban et al., 1997), *Evx1* (Bastian and Gruss, 1990; Dush and Martin, 1992), *Gbx2* (Wassarman et al., 1997), *Lef1* (Oosterwegel et al., 1993), *Bmp4* (Jones et al., 1991), *Msx1* (Hill et al., 1989), *Lh2* (Xu et al., 1993), *Fgf10* (Ohuchi et al., 1997), and *Gdf5* (Storm et al., 1994). Interestingly, all of these genes continued to be expressed distally in *Wnt5a* mutants between 10.5 d.p.c. and 12.5 d.p.c. (Fig. 7d,h and data not shown). Moreover, the *Wnt5a* expression domain itself is maintained (Fig. 7g). Finally, expression of *Shh*, which determines cell fate along the A-P axis of the limb (Riddle et al., 1993), and *Lmx1b*, which regulates D-V polarity (Riddle et al., 1995; Vogel et al., 1995), are normal in the *Wnt5a* mutants (data not shown). Our analysis demonstrates that *Wnt5a* is not required for maintenance of the AER. Moreover, the progress zone continues to express a large number of genes that are implicated in outgrowth. Finally, *Wnt5a* does not appear to regulate P-D axis outgrowth via members of the *Hoxa* or *Hoxd* complex, or indirectly through the control of genes specifying the A-P or D-V axes. One important caveat is that most of our analysis has been confined to addressing target genes at the transcriptional level but Wnt5a signalling may control one of the above genes post-transcriptionally.

### *Wnt5a* is required for the proliferation of progress zone and paraxial mesoderm progenitors

Examination of the incorporation of the nucleotide analogue 5-bromo-2'-deoxyuridine (BrdU) at 12.5 d.p.c. revealed a zone of reduced mitotic activity within the normal domain of *Wnt5a* expression suggesting that distal truncation may arise, at least in part, from decreased proliferation within the progress zone (Fig. 8a, b). To quantify the number of proliferating progress zone cells, labelled mesenchymal cells lying between the AER and the distal end of the condensing mesenchyme, were counted in multiple parallel sections. Pairwise comparisons made between stage-matched mutant and wild-type littermates ($n$=6 pairs) revealed a statistically significant decrease of 13.4% (paired Student's $t$-test, $P$<0.0001) in the number of progress zone cells that had entered S-phase in the absence of *Wnt5a*. Apparent reductions in cell densities in mutant distal limb mesenchyme were not consistently observed in mutant forelimbs and no statistically significant difference was observed in pairwise comparisons ($n$=6).

To determine whether a similar alteration of the paraxial mesoderm progenitor cell cycle could account for the reduced size of the PSM and embryonic A-P axis, we quantified wt and mutant dorsal paraxial mesoderm cells underlying the primitive streak ectoderm for incorporation of BrdU at 8.5 d.p.c. (Fig. 8c,d). A 6.8% reduction (paired Student's $t$-test, $P$<0.05) in the number of BrdU-positive caudal paraxial mesoderm cells was observed in the absence of *Wnt5a* function when compared to stage-matched wild-type littermates ($n$=3 pairs). No alterations in mutant paraxial mesoderm cell density were observed, however the morphology of the streak was consistently unusual, displaying a deep furrowing of the streak ectoderm (Fig. 8d) compared to the relatively flat ectoderm of the wild-type streak (Fig. 8c). These results are consistent with a requirement for *Wnt5a* in the developing limb and trunk for normal proliferation of mesenchymal cells of the progress zone, and primitive streak, respectively. Furthermore, we did not observe any change in

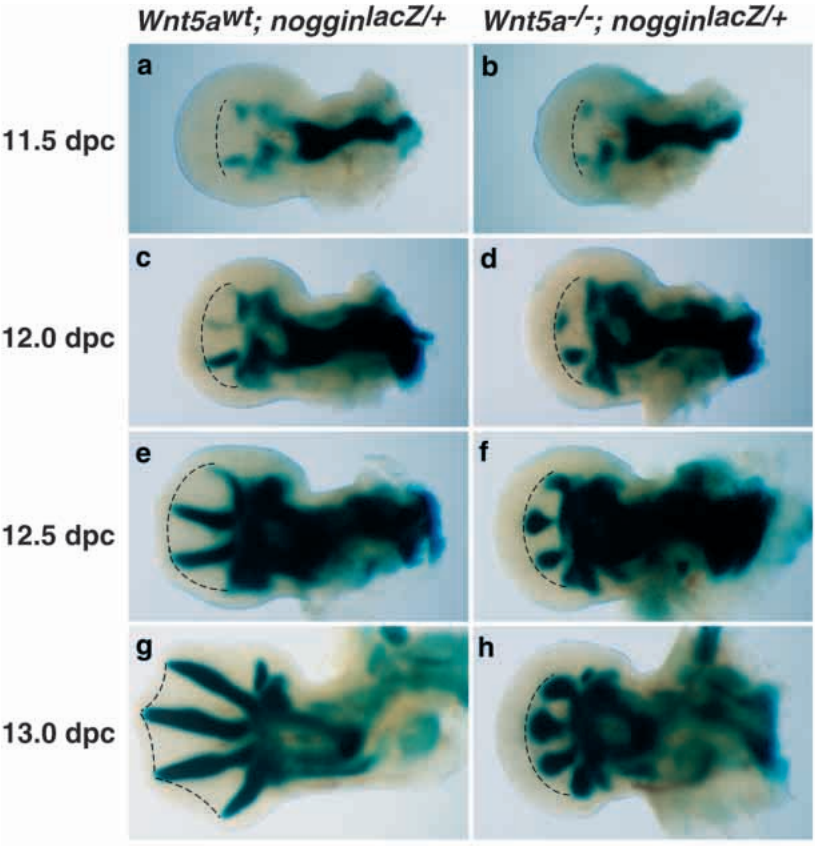


**Fig. 6.** Analysis of the ontogeny of the early forelimb skeleton primordia (11.5-13.0 d.p.c.). *Wnt5a* wild-type (a,c,e,g) and mutant (b,d,f,h) limbs expressing β-galactosidase under the control of noggin regulatory elements. The mesenchymal condensations appear to be specified properly at 11.5 d.p.c. (b) but the distal metacarpal primordia do not extend distally at 12.0 d.p.c. (d) compared to wild type (c). The lack of distal extension is more evident at later stages and is apparent in more proximal elements such as the radius and ulna at 12.5 (f) and 13.0 (h) d.p.c. The dashed lines indicate the distal extent of differentiating cells.

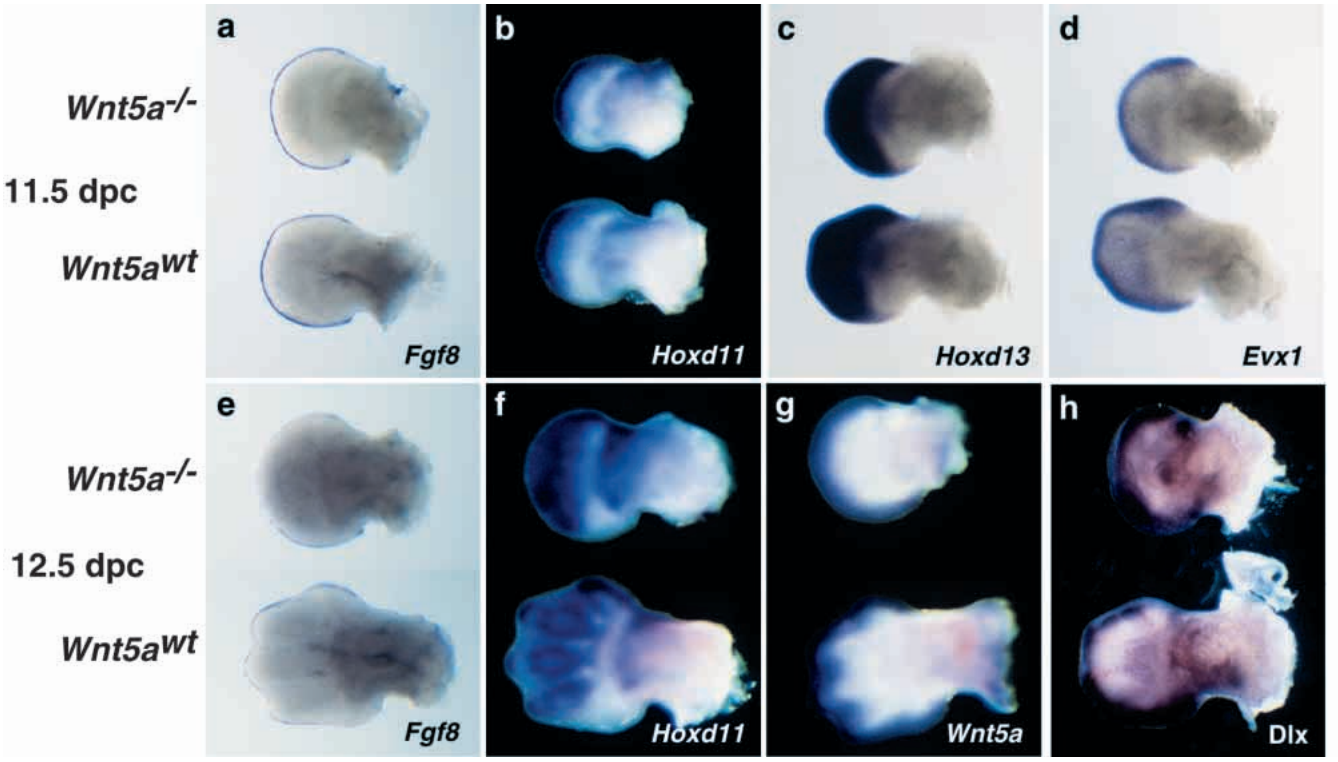


**Fig. 7.** Whole-mount in situ analysis of *Wnt5a*$^{-/-}$ 11.5-12.5 d.p.c. forelimbs. All views are of the dorsal aspect of the dissected wild-type (lower) and mutant (upper) limbs, distal to the left. (a) *Fgf8*, (b) *Hoxd11*, (c) *Hoxd13*, and (d) *Evx1* mRNA are all expressed in 11.5 d.p.c. limbs lacking *Wnt5a*. (e) *Fgf8*, (f) *Hoxd11*, (g) *Wnt5a* and (h) Dlx continue to be expressed in the mutant limbs at 12.5 d.p.c. *Wnt5a*$^{-/-}$ limbs appear to have arrested development at 11.5 d.p.c. but distal *Wnt5a*-expressing cells survive in the absence of *Wnt5a*.

apoptosis (data not shown) suggesting that *Wnt5a* may function as a mitogen, but not as a survival factor, during outgrowth of the limb and body axes.

### *Wnt5a* is essential for outgrowth of the genital tubercle

Several parallels have been drawn between the development of the limbs and that of the genital tubercle and we have shown that both express *Wnt5a* in a proximodistal gradient. Interestingly, at 18.5 d.p.c., *Wnt5a* mutant embryos lack a genital tubercle (Fig. 3h). Analysis of mutant embryos between 10.5 and 14.5 d.p.c. reveals that stunted genital tubercle outgrowths can be detected in *Wnt5a* mutants (data not shown). Furthermore, Fgf8 expression, which is normally found in the distal tip of the outgrowing genital tubercle at 10.5 d.p.c. (Fig. 5i), is observed between the hindlimbs (Fig. 5j). These results suggest that the genital primordia is specified in mutant embryos, but as in the limbs and embryonic trunk/tail, genital tubercle outgrowth is impaired in the absence of *Wnt5a*.

## DISCUSSION

The striking conclusion from this study is that proximal-distal outgrowth of diverse structures in the vertebrate embryo is controlled by a common mechanism which requires *Wnt5a* signalling.

### *Wnt5a* is required during gastrulation for morphogenesis and axis extension

We have demonstrated that *Wnt5a* is required for extension of the A-P body axis and that it is expressed at the appropriate time and place to carry out this function directly. Careful analysis of somite formation during mouse embryogenesis suggests that somitogenesis and A-P axis extension are related morphogenetic events (Tam, 1981). In other words, the length of the A-P axis correlates with the size and number of somites. Studies utilizing cultures of PSM explanted at different developmental stages, demonstrated that the size of a somite directly correlates with the size of the PSM from which it was derived (Tam, 1986), suggesting that somite size is simply dictated by the number of PSM cells available to be incorporated into a somite at the time of segmentation. In turn, maintenance of PSM size is dependent upon the primitive streak and tailbud, which function as sources of new cells to replace those committed to somite formation (Tam, 1986). The size of the PSM is therefore dictated by a balance of several processes: the removal of cells at the rostral end to form a new somite, the addition of new paraxial mesoderm cells supplied by the primitive streak or tailbud to the caudal end of the PSM, and the interstitial growth of committed somite precursors. We have shown that loss of *Wnt5a* function leads to a dramatic reduction in the A-P length of somites, PSM and primitive streak but does not affect the rate of segmentation. Since *Wnt5a* is not expressed in the forming somites themselves, we suggest that the shortened embryonic A-P axis and smaller somites

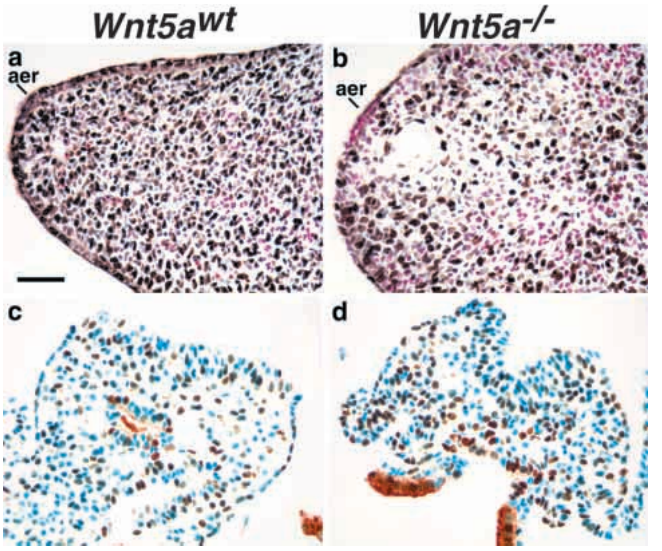


**Fig. 8.** BrdU incorporation into 12.5 d.p.c. wild-type (a) and mutant (b) forelimbs and the caudal ends of 8.5 d.p.c. wild-type (c) and mutant (d) embryos. Abbreviations: (aer) apical ectodermal ridge. Bar 50 μm.

observed in the mutants is secondary to a requirement for *Wnt5a* in the PSM and primitive streak. Taken together with our demonstration that there are fewer streak mesoderm cells in S phase in the *Wnt5a* mutant, the results suggest a model in which *Wnt5a* functions in the streak and PSM to regulate the proliferation of paraxial mesoderm progenitors.

Several cell-marking and transplantation studies investigating the fate of the primitive streak and tailbud have implied the existence of a small population of paraxial mesoderm stem cells that are capable of supplying trunk and tail mesoderm (Tam and Trainor, 1994 for review; Wilson and Beddington, 1996). Basing their hypothesis on in vivo clonal analyses, Nicolas et al. (1996) have proposed that a permanent pool of 100-150 stem cells arises in the primitive streak around 7.5 d.p.c., remains a constant size through self-renewal, and produces paraxial mesoderm progenitors capable of populating any portion of the A-P axis. The shortened primitive streak observed in *Wnt5a* mutants is detectable by 7.75-8 d.p.c., shortly after the pool of streak stem cells is proposed to arise, strongly suggesting that *Wnt5a* participates in the expansion or maintenance of this stem cell pool. *Wnt5a* probably does not function as an inducer of a mesodermal stem cell itself since all markers of mesoderm specification examined continue to be expressed in the absence of *Wnt5a*. Furthermore, a significant amount of trunk mesoderm still forms in mutant embryos.

Our hypothesis provides an explanation for the differing requirements for *Wnt5a* in primary and secondary body formation. We propose that during primary body formation, the source of cells at the caudal end of the PSM is generated through two related mechanisms; a *Wnt5a*-independent mechanism that induces mesodermal stem cells in the primitive streak, and a *Wnt5a*-dependent mechanism that regulates the division of these stem cells. In the absence of *Wnt5a*, new mesodermal stem cells can still develop in the primitive streak but their ability to divide and give rise to progeny (both stem cells and progenitor cells) may be compromised. For instance, a lengthening of the cell cycle would lead to the generation of fewer somitic progenitors with time and could manifest in a progressive reduction in somite size along the rostral-caudal axis as is observed in *Wnt5a* mutants. The caudal tailbud stem cells responsible for secondary body formation are direct descendants of primitive streak stem cells (Tam and Tan, 1992; Wilson et al., 1995) and are likely maintained through self-renewal since ingression of ectodermal cells no longer occurs at these stages. Thus, a depletion of streak-derived stem cells in the mutant tailbud, in conjunction with a failure to maintain stem cells in the tailbud, may lead to axial truncation as observed in *Wnt5a* mutants.

Our data are consistent with Pasteels proposal that secondary body formation is essentially a continuation of the gastrulation process responsible for primary body formation (Pasteels, 1943). Further support has accumulated recently from the analysis of gene expression data and fate maps in the frog, chick, mouse and zebrafish (Catala et al., 1995; Gont et al., 1993; Kanki and Ho, 1997; Tam and Tan, 1992; Wilson and Beddington, 1996). These studies suggest that in vertebrates the generation of mesoderm by ingression during gastrulation or in situ by the tailbud are similar and related processes. Further evidence comes from analysis of *pipetail* mutants in the zebrafish (Rauch et al., 1997). *Pipetail* is most likely a *Wnt5a* allele which results in defective tail development. Given that *Wnt5a* is expressed at the caudal end of all vertebrate embryos examined to date (Dealy et al., 1993; Moon et al., 1993a; Rauch et al., 1997), it seems likely that *Wnt5a* plays a conserved role in axis extension and tail development throughout the vertebrate phylum.

### *Wnt5a* regulates proliferation of limb progenitors in the progress zone

In the limb, *Wnt5a* is essential for proper outgrowth and, consequently patterning, along the P-D axis. The role of AER signals in regulating outgrowth and P-D patterning is well established. Heterochronic transplants of the AER indicate that it plays a supportive and not instructive role (Saunders and Reuss, 1974), and removal of the AER results in the development of limbs that are truncated at a precise position along the P-D axis defined by the time of AER removal (Saunders, 1948). Structures proximal to this position develop normally. In *Wnt5a* mutants, the AER appears normal. Moreover, the phenotype is progressive rather than absolute. Thus, it is unlikely that *Wnt5a* is required for AER activity. However, the decreased proliferation observed in the progress zone suggests that *Wnt5a* could mediate some of Fgfs mitogenic activity in the progress zone. Alternatively, Wnt5a may function together with Fgfs in a synergistic fashion to regulate distal mesenchymal cell proliferation. It is tempting to speculate that the transcriptional gradient of *Wnt5a* mRNA in the progress zone is established by diffusion of an Fgf(s) expressed by the AER.

The progress zone model was developed to explain how pattern can be specified in a growing tissue (Summerbell et al., 1973). It requires three principal components to specify positional information in an outgrowing structure: (1) a positional value(s), (2) a positional signal, and (3) cell division. *Wnt5a* is expressed in the progress zone during all stages of limb outgrowth and is therefore a candidate for any of these

components. Markers of proximal and distal positional information are unperturbed in the absence of *Wnt5a*, suggesting that it does not play a role in specification of these values. Furthermore, *Wnt5a* is not likely to be the positional signal that defines the size of the progress zone since the model would predict that if the size of the progress zone was reduced then the initial size of the skeletal primordia would be proportionately reduced and this was not observed in the *Wnt5a* mutants. The fact that there are fewer cycling cells in the progress zone argues that *Wnt5a* functions here, as in the primitive streak and tailbud, to regulate the division of mesenchymal progenitors.

Analysis of the fates of chick limb cells demonstrated that the P-D expansion of mesenchymal cells labelled subapically (ie. distally in the progress zone) was several-fold greater than those labelled in more proximal positions (Vargesson et al., 1997). Labelled subapical cells always remained closely associated with the apical ridge demonstrating that a population of labelled progenitor cells remained in the progress zone and gave rise to progeny that were distributed along a large portion of the P-D axis. These results are similar to those described earlier for the fate of labelled streak and tailbud cells (see above). In our model for limb outgrowth, signals from the AER specify limb progenitor cells through a *Wnt5a*-independent mechanism. *Wnt5a* subsequently functions in the progress zone to regulate the proliferation of these limb progenitor cells in a fashion analagous to that proposed above for the regulation of paraxial mesoderm stem cells by *Wnt5a*. In the absence of *Wnt5a*, progenitor cells undergo fewer total cell divisions. This would lead to a progressive reduction in the number of progeny capable of differentiating over time ultimately resulting in insufficient numbers of cells to generate distal skeletal primordia. The impairment of progenitor cells to divide and give rise to another progenitor cell or a differentiating cell could explain the apparently static population of β-gal-negative cells observed in the mutant progress zone even though distal positional information continues to be expressed at this time.

### A common mechanism may underly tissue outgrowth

The number of somites and vertebrae vary enormously between vertebrate species however the mechanisms governing evolutionary changes in somite number is unknown (Richardson et al., 1998 for review). Tam (1981) has proposed that control of somite number could be achieved through regulation of progenitor cell proliferation. Cells destined for more caudal somites could be generated by increasing the number of progenitor cell divisions. Since vertebrate segmentation appears to be open-ended (Richardson et al., 1998) ie. segmentation may continue as long as a threshold number of cells are present, then regulation of somite number could be achieved by simply regulating the pool of progenitor cells available for segmentation. It is interesting to note that the formation of skeletal primordia during limb development also requires a threshold number of cells (Wolpert et al., 1979). Moreover, a relationship between the number of skeletal elements and the number of cell divisions the progress zone limb progenitors undergo has been proposed (Lewis, 1975). These similarities suggest that regulation of the size of a progenitor cell pool could be sufficient to regulate both somite number and limb length and that a common developmental mechanism may govern these processes.

Our demonstration that the number of cycling limb and somite progenitors is reduced in *Wnt5a* mutants provides further support for this hypothesis. While the numerical differences are small, they are nevertheless significant, especially when considering that the average cell cycle of ectoderm and mesoderm cells of the gastrulating embryo is 7.5 hours, and as short as 3 hours in the primitive streak (Lawson et al., 1991; MacAuley et al., 1993; Snow, 1977). We suggest that subtle modulations of cell cycle times of rapidly dividing progenitors may be sufficient to account for the dramatic phenotypic consequences caused by a loss-of-function mutation in *Wnt5a*. However, we cannot rule out the possibility that *Wnt5a* regulates other additional cellular processes such as cell adhesion (Moon et al., 1993a,b) or cell polarity (Shulman et al., 1998).

A common mechanism has also been inferred for the regulation of limb and genital outgrowth since loss of posterior Hox gene function results in a loss of digits and the genital tubercle (Kondo et al., 1997). These authors have proposed that the evolutionary emergence of digits could have arisen from the acquisition of distal *Hoxd* expression leading to an extension of limb progenitor proliferation (Sordino et al., 1995). While it is unclear at this moment whether a relationship between the posterior Hox genes and *Wnt5a* exists it is tempting to speculate that *Wnt5a* lies downstream of them. Our demonstration that a single gene can regulate the outgrowth of the embryonic axis and the facial, genital, ear and limb primordia suggest that the latter evolutionarily adaptive structures that grew out from the main body axis could have arisen from modifications of the same genetic program responsible for elaboration of the primary body plan.

We are very grateful to S. Lee and B. St.-Jacques for providing tissue section in situ hybridization data. We would like to thank A. R. Hancock, D. Faria and B. Klumpar for excellent technical assistance, and T. Calzonetti, P.-T. Chuang, J. Cygan, S. Karp, P. Lewis and Y. Yang for critically reading the manuscript. We thank S. Carroll, D. Duboule, R. Grosschedl, J. C. Izpisua-Belmonte, R. Johnson, G. Martin, and V. Papaioannou for providing some of the probes used in these studies. T. P. Y. was supported by postdoctoral fellowships from the Human Frontiers Science Program and the Medical Research Council of Canada. Work in A. P. M.'s laboratory is supported by a grant from the NIH.

## REFERENCES

**Bastian, H. and Gruss, P.** (1990). A murine even-skipped homologue, Evx 1, is expressed during early embryogenesis and neurogenesis in a biphasic manner. *EMBO J.* **9,** 1839-1852.

**Beddington, R. S.** (1994). Induction of a second neural axis by the mouse node. *Development* **120,** 613-620.

**Bettenhausen, B., Hrabe de Angelis, M., Simon, D., Guenet, J. L. and Gossler, A.** (1995). Transient and restricted expression during mouse embryogenesis of Dll1, a murine gene closely related to Drosophila Delta. *Development* **121,** 2407-2418.

**Brunet, L. J., McMahon, J. A., McMahon, A. P. and Harland, R. M.** (1998). Noggin, cartilage morphogenesis, and joint formation in the mammalian skeleton. *Science* **280,** 1455-1457.

**Capecchi, M. R.** (1997). Hox genes and mammalian development. *Cold Spring Harb. Symp. Quant. Biol.* **62,** 273-281.

**Catala, M., Teillet, M. A. and Le Douarin, N. M.** (1995). Organization and

development of the tail bud analyzed with the quail-chick chimaera system. *Mech. Dev.* **51,** 51-65.

**Chapman, D. L. and Papaioannou, V. E.** (1998). Three neural tubes in mouse embryos with mutations in the T-box gene Tbx6. *Nature* **391,** 695-697.

**Clevers, H. and van de Wetering, M.** (1997). TCF/LEF factor earn their wings. *Trends Genet* **13,** 485-489.

**Conlon, R. A., Reaume, A. G. and Rossant, J.** (1995). Notch1 is required for the coordinate segmentation of somites. *Development* **121,** 1533-1545.

**Crossley, P. H. and Martin, G. R.** (1995). The mouse Fgf8 gene encodes a family of polypeptides and is expressed in regions that direct outgrowth and patterning in the developing embryo. *Development* **121,** 439-451.

**Crossley, P. H., Minowada, G., MacArthur, C. A. and Martin, G. R.** (1996). Roles for FGF8 in the induction, initiation, and maintenance of chick limb development. *Cell* **84,** 127-136.

**Davis, A. P., Witte, D. P., Hsieh, L. H., Potter, S. S. and Capecchi, M. R.** (1995). Absence of radius and ulna in mice lacking hoxa-11 and hoxd-11. *Nature* **375,** 791-795.

**Dealy, C. N., Roth, A., Ferrari, D., Brown, A. M. and Kosher, R. A.** (1993). Wnt-5a and Wnt-7a are expressed in the developing chick limb bud in a manner suggesting roles in pattern formation along the proximodistal and dorsoventral axes. *Mech. Dev.* **43,** 175-186.

**Dolle, P., Dierich, A., LeMeur, M., Schimmang, T., Schuhbaur, B., Chambon, P. and Duboule, D.** (1993). Disruption of the Hoxd-13 gene induces localized heterochrony leading to mice with neotenic limbs. *Cell* **75,** 431-441.

**Dush, M. K. and Martin, G. R.** (1992). Analysis of mouse Evx genes: Evx-1 displays graded expression in the primitive streak. *Dev. Biol.* **151,** 273-287.

**Fromental, R. C., Warot, X., Messadecq, N., LeMeur, M., Dolle, P. and Chambon, P.** (1996). Hoxa-13 and Hoxd-13 play a crucial role in the patterning of the limb autopod. *Development* **122,** 2997-3011.

**Gavin, B. J., McMahon, J. A. and McMahon, A. P.** (1990). Expression of multiple novel Wnt-1/int-1-related genes during fetal and adult mouse development. *Genes Dev.* 2319-2332.

**Gont, L. K., Steinbeisser, H., Blumberg, B. and de, R. E.** (1993). Tail formation as a continuation of gastrulation: the multiple cell populations of the Xenopus tailbud derive from the late blastopore lip. *Development* **119,** 991-1004.

**Hill, R. E., Jones, P. F., Rees, A. R., Sime, C. M., Justice, M. J., Copeland, N. G., Jenkins, N. A., Graham, E. and Davidson, D. R.** (1989). A new family of mouse homeo box-containing genes: molecular structure, chromosomal location, and developmental expression of Hox-7.1. *Genes Dev.* **3,** 26-37.

**Johnson, R. L. and Tabin, C. J.** (1997). Molecular models for vertebrate limb development. *Cell* **90,** 979-990.

**Johnston, S. H., Rauskolb, C., Wilson, R., Prabhakaran, B., Irvine, K. D. and Vogt, T. F.** (1997). A family of mammalian *Fringe* genes implicated in boundary determination and the *Notch* pathway. *Development* **124,** 2245-2254.

**Jones, C. M., Lyons, K. M. and Hogan, B. L.** (1991). Involvement of Bone Morphogenetic Protein-4 (BMP-4) and Vgr-1 in morphogenesis and neurogenesis in the mouse. *Development* **111,** 531-542.

**Kanki, J. P. and Ho, R. K.** (1997). The development of the posterior body in zebrafish. *Development* **124,** 881-93.

**Kondo, T., Zakany, J., Innis, J. W. and Duboule, D.** (1997). Of fingers, toes and penises. *Nature* **390,** 29.

**Kaufman, M. H.** (1992). *The Atlas of Mouse Development*. London: Academic Press Limited.

**Lawson, K. A., Meneses, J. J. and Pedersen, R. A.** (1991). Clonal analysis of epiblast fate during germ layer formation in the mouse embryo. *Development* **113,** 891-911.

**Lewis, J. H.** (1975). Fate maps and the pattern of cell division: a calculation for the chick wing-bud. *J. Embryol. Exp. Morphol.* **33,** 419-434.

**MacAuley, A., Werb, Z. and PE, M.** (1993). Characterization of the unusually rapid cell cycles during rat gastrulation. *Development* **117,** 8738-83.

**Meyers, E. N., Lewandoski, M. and Martin, G. R.** (1998). An Fgf8 mutant allelic series generated by Cre- and Flp-mediated recombination. *Nat. Genet.* **18,** 136-141.

**Moon, R., Brown, J. and Torres, M.** (1997). WNTs modulate cell fate and behavior during vertebrate development. *Trends Genet* **13,** 1571-62.

**Moon, R. T., Campbell, R. M., Christian, J. L., McGrew, L. L., Shih, J. and Fraser, S.** (1993a). Xwnt-5A: a maternal Wnt that affects morphogenetic movements after overexpression in embryos of *Xenopus laevis*. *Development* **119,** 97-111.

**Moon, R. T., DeMarais, A. and Olson, D. J.** (1993b). Responses to Wnt signals in vertebrate embryos may involve changes in cell adhesion and cell movement. *J. Cell Sci. Suppl.* **17,** 183-188.

**Nicolas, J. F., Mathis, L., Bonnerot, C. and Saurin, W.** (1996). Evidence in the mouse for self-renewing stem cells in the formation of a segmented longitudinal structure, the myotome. *Development* **122,** 2933-2946.

**Niswander, L. and Martin, G. R.** (1992). Fgf-4 expression during gastrulation, myogenesis, limb and tooth development in the mouse. *Development* **114,** 755-768.

**Nowakowski, R. S., Lewin, S. B. and Miller, M. W.** (1989). Bromodeoxyuridine immunohistochemical determination of the lengths of the cell cycle and the DNA-synthetic phase for an anatomically defined population. *J. Neurocytol.* **18,** 311-318.

**Ohuchi, H., Nakagawa, T., Yamamoto, A., Araga, A., Ohata, T., Ishimaru, Y., Yoshioka, H., Kuwana, T., Nohno, T., Yamasaki, M., Itoh, N. and Noji, S.** (1997). The mesenchymal factor, FGF10, initiates and maintains the outgrowth of the chick limb bud through interaction with FGF8, an apical ectodermal factor. *Development* **124,** 2235-2244.

**Oosterwegel, M., van, de, Wetering, M, Timmerman, J., Kruisbeek, A., Destree, O., Meijlink, F. and Clevers, H.** (1993). Differential expression of the HMG box factors TCF-1 and LEF-1 during murine embryogenesis. *Development* **118,** 439-48.

**Panganiban, G., Irvine, S. M., Lowe, C., Roehl, H., Corley, L. S., Sherbon, B., Grenier, J. K., Fallon, J. F., Kimble, J., Walker, M., Wray, G. A., Swalla, B. J., Martindale, M. Q. and Carroll, S. B.** (1997). The origin and evolution of animal appendages. *Proc. Natl. Acad. Sci. USA* **94,** 5162-5166.

**Parr, B. A. and McMahon, A. P.** (1995). Dorsalizing signal Wnt-7a required for normal polarity of D-V and A-P axes of mouse limb. *Nature* **374,** 350-353.

**Parr, B. A., Shea, M. J., Vassileva, G. and McMahon, A. P.** (1993). Mouse Wnt genes exhibit discrete domains of expression in the early embryonic CNS and limb buds. *Development* **119,** 247-261.

**Pasteels, J.** (1943). Proliferations et croissance dans la gastrulation et la formation de la queue des Vertebres. *Arch. Biol.* **54,** 1-51.

**Rauch, G. J., Hammerschmidt, M., Blader, P., Schauerte, H. E., Strahle, U., Ingham, P. W., McMahon, A. P. and Haffter, P.** (1997). Wnt5 is required for tail formation in the zebrafish embryo. *Cold Spring Harb. Symp. Quant. Biol.* **62,** 227-234.

**Richardson, M. K., Allen, S. P., Wright, G. M., Raynaud, A. and Hanken, J.** (1998). Somite number and vertebrate evolution. *Development* **125,** 151-160.

**Riddle, R. D., Ensini, M., Nelson, C., Tsuchida, T., Jessell, T. M. and Tabin, C.** (1995). Induction of the LIM homeobox gene Lmx1 by WNT7a establishes dorsoventral pattern in the vertebrate limb. *Cell* **83,** 631-40.

**Riddle, R. D., Johnson, R. L., Laufer, E. and Tabin, C.** (1993). Sonic hedgehog mediates the polarizing activity of the ZPA. *Cell* **75,** 1401-1416.

**Saunders, J. J. and Reuss, C.** (1974). Inductive and axial properties of prospective wing-bud mesoderm in the chick embryo. *Dev Biol* **38,** 41-50.

**Saunders, J. W., Jr.** (1948). The proximo-distal sequence of origin of the parts of the chick wing and the role of the ectoderm. *J. Exp. Zool.* **108,** 363-403.

**Shulman, J., perrimon, N. and Axelrod, J.** (1998). Frizzled signalling and the developmental control of cell polarity. *Trends Genet* **14,** 452-458.

**Slusarski, D., Corces, V. and RT, M.** (1997). Interaction of Wnt and a Frizzled homologue triggers G-protein-linked phosphatidylinositol signalling. *Nature* **390,** 410-413.

**Snow, M. H. L.** (1977). Gastrulation in the mouse: growth and regionalization of the epiblast. *J. Embryol. exp Morph.* **42,** 293-303.

**Sordino, P., van, der, Hoeven, F and Duboule, D.** (1995). Hox gene expression in teleost fins and the origin of vertebrate digits. *Nature* **375,** 678-81.

**Storm, E. E., Huynh, T. V., Copeland, N. G., Jenkins, N. A., Kingsley, D. M. and Lee, S. J.** (1994). Limb alterations in brachypodism mice due to mutations in a new member of the TGF beta-superfamily. *Nature* **368,** 639-643.

**Summerbell, D., Lewis, J. H. and Wolpert, L.** (1973). Positional information in chick limb morphogenesis. *Nature* **244,** 492-496.

**Takada, S., Stark, K. L., Shea, M. J., Vassileva, G., McMahon, J. A. and McMahon, A. P.** (1994). Wnt-3a regulates somite and tailbud formation in the mouse embryo. *Genes Dev.* **8,** 174-189.

**Tam, P. P.** (1981). The control of somitogenesis in mouse embryos. *J. Embryol. Exp. Morphol.* **65 Suppl.,** 103-128.

**Tam, P. P.** (1986). A study of the pattern of prospective somites in the

presomitic mesoderm of mouse embryos. *J. Embryol. Exp. Morphol.* **92,** 269-285.

**Tam, P. P.** (1989). Regionalisation of the mouse embryonic ectoderm: allocation of prospective ectodermal tissues during gastrulation. *Development* **107,** 55-67.

**Tam, P. P. and Tan, S. S.** (1992). The somitogenetic potential of cells in the primitive streak and the tail bud of the organogenesis-stage mouse embryo. *Development* **115,** 703-715.

**Tam, P. P. and Trainor, P. A.** (1994). Specification and segmentation of the paraxial mesoderm. *Anat. Embryol. (Berl)* **189,** 275-305.

**Vargesson, N., Clarke, J. D., Vincent, K., Coles, C., Wolpert, L. and Tickle, C.** (1997). Cell fate in the chick limb bud and relationship to gene expression. *Development* **124,** 1909-1918.

**Vogel, A., Rodriguez, C., Warnken, W. and Izpisua, B. J.** (1995). Dorsal cell fate specified by chick Lmx1 during vertebrate limb development. *Nature* **378,** 716-720.

**Wassarman, K. M., Lewandoski, M., Campbell, K., Joyner, A. L., Rubenstein, J. L., Martinez, S. and Martin, G. R.** (1997). Specification of the anterior hindbrain and establishment of a normal mid/hindbrain organizer is dependent on Gbx2 gene function. *Development* **124,** 2923-2934.

**Whiting, J., Marshall, H., Cook, M., Krumlauf, R., Rigby, P. W., Stott, D. and Allemann, R. K.** (1991). Multiple spatially specific enhancers are required to reconstruct the pattern of Hox-2.6 gene expression. *Genes Dev.* **5,** 2048-2059.

**Wilkinson, D. G. and Nieto, M. A.** (1993). Detection of messenger RNA by in situ hybridization to tissue sections and whole mounts. *Methods Enzymol.* **225,** 361-73.

**Wilson, V. and Beddington, R. S.** (1996). Cell fate and morphogenetic movement in the late mouse primitive streak. *Mech. Dev.* **55,** 79-89.

**Wilson, V., Manson, L., Skarnes, W. C. and Beddington, R. S.** (1995). The T gene is necessary for normal mesodermal morphogenetic cell movements during gastrulation. *Development* **121,** 877-886.

**Winnier, G., Blessing, M., Labosky, P. A. and Hogan, B. L.** (1995). Bone morphogenetic protein-4 is required for mesoderm formation and patterning in the mouse. *Genes Dev.* **9,** 2105-2116.

**Wolpert, L., Tickle, C. and Sampford, M.** (1979). The effect of cell killing by x-irradiation on pattern formation in the chick limb. *J. Embryol. Exp. Morphol.* **50,** 175-193.

**Xu, Y., Baldassare, M., Fisher, P., Rathbun, G., Oltz, E. M., Yancopoulos, G. D., Jessell, T. M. and Alt, F. W.** (1993). LH-2: a LIM/homeodomain gene expressed in developing lymphocytes and neural cells. *Proc. Natl. Acad. Sci. USA* **90,** 227-231.